

### Study of the High Rotational Bands of Moderately Heavy Nuclei

F. Z. Hamel and D. E. Medjadi

*Laboratoire N-corps et Structure de la Matière, Ecole Normale Supérieure, Kouba, 16050  
Alger, Algeria.*

**Doi:** <https://doi.org/10.47011/15.5.5>

*Received on:* 28/02/2021;

*Accepted on:* 30/05/2021

---

**Abstract:** This paper provides a study of the rotational properties of heavy and medium nuclei, particularly the paired nuclei existing in the rare-earth, including Gd, Er, ..., first to have a good representation of the intrinsic prolate fundamentals of the considered nuclei. The most important residual nuclear interaction is the pairing force which makes it possible to couple the nucleons in pairs. To take it into account, we introduce the Bardeen-Cooper-Shrie formalism (BCS), developed to describe the phenomenon of superconductivity. The test wave function is then more elaborate than that of Hartree-Fock and corresponds to a state no longer of independent particles, but of independent quasi-particles. A quasi-particle state (qp) is a linear combination of particles and holes. The Routhian Hartree-Fock model through the analysis of the experimental spectra of rotation of the deformed nucleus was used. Knowing that this was originally expanded by Bohr-Mottelson by applying  $I(I+1)$  expansion, we modified an existing fixed code (HF) with axial symmetry, which extended in a way that allows us to add constraints on the angular momentum and kelvin rotation to the Hamiltonian known as Cr.HF (cranking version of this formalism), initially studied by P. Quentin. This modification led to good results, especially the spectra of rotation and the angular velocities as a function of the angular momentum. Besides, it led to a decrease in the moment of inertia after it was large in some models, such as in the Hartree-Fock-Bogoliubov (HFB) model. The rotational properties and the moments of inertia of the super-deformed bands of some deformed nuclei have been studied as well as in the mass regions  $A=190$ ;  $A=160$ . The results were compared with experimental results which gave good agreement. This work will offer an interesting perspective necessary for certain improvements or extensions of the Cr.HF.

**Keywords:** Microscopic mean field, Collective nuclear rotation, Angular momentum Routhian Hartree-Fock (RHF) model, Inertia moments, Angular velocity.

## 1. Introduction

An important part of nuclear physics is dedicated to models attempting to explain the growing mass of experimental results. At present, the nuclear forces, although "identified" in their entirety, have not definitively disclosed all their secrets. We need then models to explain how an atomic nucleus is constituted, why it is stable or unstable and what its characteristics are. We call this part of nuclear physics the nuclear structure. By discovering the exotic nuclei, the nuclear structure has become more

complicated although the computational means are at present also more important and the models are more efficient. One of the most important concepts of nuclear structure is the deformation of nuclei [1]. This means that the nuclear surface in the ground state (equilibrium) is a surface that is no longer spherical. In addition, all phenomena are associated with the dynamics of the nuclear surface, such as: nuclear fission, nuclear fission, collective bands of rotation and vibration, quadrupole moments and

many other phenomena naturally embedded in this notion.

Physics has constantly tried to explain the structure of nuclei and the phenomena that involve them in terms of their basic constituents "nucleons" and their mutual interactions. Such a "microscopic" description of nuclei obviously has many advantages, since it provides a unified framework allowing in principle to deduce the properties of all imaginable nuclear systems. In a few words, the situation is as follows: BCS theory [2], where the different states are described as quasi-particles (free quasi-particle model) excitations on a vacuum which is the ground state of the nucleus, trying to describe the structure of nuclei and their isomeric states.

There are many models in the microscopic calculations, especially in the calculation of the rotational-energy spectrum and its variation in terms of angular momentum, as well as in the calculation of the kinetic moment in which the researchers attempted to reduce it. Initially, it was discussed particularly at a relatively low angular momentum called the Coriolis anti-pairing effect. It was studied in terms of coupling rotation - group coupling by Mottelson Valatin [3] [4].

Thanks the generalized Routhian approximation, we have developed a quantum microscopic formalism with an average harmonic oscillator field that remarkably reproduces the results of the phenomenological models previously discussed. Subsequently, we have constructed and tested the validity of a realistic microscopic and self-consistent code of Hartree-Fock type, where we describe the interactions between the nucleons by the phenomenological force of Skyrme to study the S-type ellipsoids to the approximation of the generalized cranking.

In this paper, we discuss the use of the Routhian Hartree-Fock method for isotopes of the nuclei Hg, Pb and A=160, using the Routhian approximation in which we add a constraint on the moment of inertia through finding a new equation between global rotation and intrinsic vorticity.

The paper is organized as follows. In Sections 1, 2 and 3, we dealt with a definition of the BCS model, which has a good base, in order to study the static properties of some paired nuclei, while In Sections 4 and 5, within the framework of the

independent-particle approximation that is used to describe the nuclei formal dynamics (based on Schrödinger's equation), we have chosen to develop a realistic microscopic description of the S-type ellipsoids using the Hartree-Fock approximation. This work consisted of modifying an existing fixed code with axial symmetry by adding constraints on the angular momentum and the kelvin rotation to the approximation of the general cranking. In section 6, we present and discuss the angular velocity and calculations related to angular momentum and rotational-energy spectrum, Section 7 is devoted to studying in detail the rotational-band model, where we have determined some rotational properties; i.e., the rotational band, the angular momentum, the rotational speed and comparing the results with the experimental data, together with some conclusions and perspectives offered by this new approach.

## 2. The Ground-state BCS

We now present a method, inspired by the BCS theory in solid state physics [5], which takes into account correlations (particle-particle). This method will not give an exact solution for the eigenvalue problem, but will establish solutions from a variational principle. Formally, we will follow the same approach as that applied in the Hartree-Fock method; we choose a family of test states and minimize the energy. This also leads us to introduce the notion of quasi-particle using the Bogoliubov transformation. The idea now is to see the system of interacting particles as a system of independent quasi-particles moving in an average potential, which in this case is the pairing potential. According to the BCS theory, we can choose the test state of a kernel (pair-pair) for example, as shown in the following form:

$$\psi |BCS\rangle = \prod_{k>0} (u_k + v_k a_k^\dagger a_{\bar{k}}^\dagger) |0\rangle \quad (1)$$

where  $v_k$  and  $u_k$  are complex parameters and the product spans all values of  $k$  in half the configuration space; therefore, for each state  $k > 0$ , there exists a state reversed with respect to time  $k < 0$  such that the state  $\{k, \bar{k}\}$  generates all the mono-particulate space. Thus, we notice that the one-particle states  $k$  and  $\bar{k}$  are grouped in pairs [6]; they are simultaneously occupied or unoccupied. The variational principle determines the parameters  $u_k$  and  $v_k$  which are not independent and satisfy the relation.

### 3. BCS Equations

Using the Bogoliubov transformation, we obtained a representation of the test state of particles interacting in pairs in terms of a non-interacting quasi-particle gas. There is a spontaneous breaking of the particle number symmetry, because this transformation mixes the operators of creation and annihilation, so that the number of particles is not conserved. We introduce a Lagrange parameter which fixes the average number of particles to its exact value in order to perform energy minimization, which is equivalent to solving an eigenvalue problem. We will therefore have the constrained Hamiltonian in the form:

$$H' = H - \lambda \hat{N} \quad (2)$$

$\lambda$  is the Lagrange parameter, which is interpreted as a chemical potential or Fermi energy, since it represents the change in energy

$$E = \langle \psi_{BCS} | H' | \psi_{BCS} \rangle, \quad (3)$$

with respect to the variation in the number of particles [7]:

$$\lambda = \frac{dE}{dN}. \quad (4)$$

According to the definition of the wave function  $|\psi_{BCS}\rangle$ , the Hamiltonian  $H'$  takes the form:

$$E = \langle \psi_{BCS} | H | \psi_{BCS} \rangle. \quad (5)$$

First, the basic case is studied by finding the minimum energy and the corresponding quadrupole moment by using a program and since the results obtained on it for the quadrupole moment, we enter the parameters in the Routhien program that gives us the results to determine a good  $\Omega$ .

### 4. Hamiltonian Symmetries

The Routhian in the context of generalized cranking at the coupling of S-type ellipsoids is simply written in the form:

$$H = H_{SKY} - \Omega \hat{J}_1 - \omega(\Omega) \hat{K}_1, \quad (6)$$

where  $H_{SKY}$  stands for the Skyrme Hamiltonian [8-10]. As well,  $\hat{K}_1$  is the Kelvin's circulation operator.

$$\hat{J}_1 = \hat{L}_1 + \hat{S}_1, \quad (7)$$

$\hat{J}_1$  is the total angular momentum operator that combines both the spin and orbital angular

momentum operators. The Skyrme Hamiltonian is invariant by the parity operation that consists of replacing the coordinates and the momentum of the system by their opposites. Besides, it is easy to see that the operators  $\hat{L}_1, \hat{K}_1$  consist of the product of momentum by coordinates; they are also invariant by this operation [11].

### 5. Functional Energy

E. Chabanat *et al.* [12] showed that a Skyrme interaction is given by the following expression:

$$\langle \emptyset | \hat{H} | \emptyset \rangle = \int d^3 r H_{\text{totale}}, \quad (8)$$

with

$$H_{\text{totale}}(r) = H_{SK}(r) + H_{Coul}(r), \quad (9)$$

where the total energy density  $H_{\text{totale}}(r)$  is the sum of the density related to the Skyrme force and that related to Coulomb energy, while the energy of Slater's determinant is calculated as:

$$E_{HF} = \int dr H_{\text{totale}}. \quad (10)$$

This Hamiltonian density is a functional one-body density (diagonal matrix elements in  $\vec{r}$  of  $\vec{p}$ ), which for a determinant of even Slater by reversal of the sense of time can in a somewhat arbitrary way be decomposed as:

$$H_{SK}(r) = H_{kin}(r) + H_{vol}(r) + H_{surf}(r) + H_{so}(r), \quad (11)$$

The different terms of the above equation depend on a certain number of local densities. The spin-vector and the current densities are not involved for even solutions by reversing the time direction. This is the reason why we will not consider them to describe the fundamental states of even-peer nuclei. We should only consider the densities of matter, kinetic energy and spin-orbit from the wave functions and the determinant of Slater, respectively. The normal density of the nucleus is:

$$\rho(r) = \sum_{i,\sigma} |\phi_i(r, \sigma)|^2. \quad (12)$$

The density of normal kinetic energy (scalar spin) is given by:

$$\tau(r) = \sum_{i,\sigma} \vec{\nabla} |\phi_i(r, \sigma)|^2, \quad (13)$$

and the spin-orbit density is:

$$\vec{j}(r) = (-i) \sum_{i,\sigma,\sigma'} \phi_i^*(r, \sigma) [\vec{\nabla} \phi_i(r, \sigma) \times \langle \sigma | \vec{\sigma} | \sigma' \rangle]. \quad (14)$$

Here the summations  $i$  (space) and  $\sigma, \sigma'$  (spin) concern all the occupied states of a particle and  $\tau$  stands for the different states of charge (neutrons ( $n$ ) and protons ( $p$ )). In what follows, the isospin index  $\tau$  affects densities, so that the summations on the indices  $i$  and  $j$  only imply state densities having even isospin  $\tau$ . The densities noted without indices  $\tau$  are equal to the sum of the corresponding neutron and proton densities:

$$H_{\text{kin}} = \frac{A-1}{A} \frac{\hbar^2}{2m} \tau, \quad (15)$$

$$H_{\text{vol}}(r) = B_1 (\rho)^2 + B_2 \sum_q (\rho)^2 + B_3 \rho \tau + B_4 \sum_q \rho_q \tau_q + B_7 \rho^{a+2} + B_8 \rho^a \sum_q \rho_q^2, \quad (16)$$

$$H_{\text{surf}}(r) = B_5 \rho \vec{\nabla}^2 \rho + B_6 \sum_q \rho_q \vec{\nabla}^2 \rho_q, \quad (17)$$

$$H_{\text{so}}(r) = B_9 (\rho \vec{\nabla} \cdot \vec{J} + \sum_q \rho_q \vec{\nabla} \cdot \vec{J}_q), \quad (18)$$

where the dependency in  $\vec{r}$  of the different densities is implied [13,14]. The coefficient  $(A-1)/A$  Eq. (10) of the kinetic energy functional results from the subtraction of the part to a body of energy due to the movement of the center of mass, with  $A$  being the number of nucleons of the nucleus. The coefficients  $B_i$  of the Skyrme force are summarized in the table shown in [15]. To take into account the Coulombian interaction, which is not included in the Skyrme interaction, it is necessary to add to the energy functional the Coulombian energy functional, which can be written using Slater's approximation for the exchange term in the form:

$$H_{\text{Coul}}(r) = \frac{1}{2} \rho_p V_{\text{Coul}} - \frac{3}{4} e^2 4 \left(\frac{3}{\pi}\right)^{\frac{1}{3}} (\rho_p)^{\frac{4}{3}}, \quad (19)$$

where  $e$  is the proton charge,  $\rho_p$  [16] is the proton density and the potential  $V_{\text{Coul}}$  is expressed by:

$$V_{\text{Coul}} = e^2 \int d^3 r' \frac{\rho_p(r')}{|r-r'|}. \quad (20)$$

Moreover, the exchange term can be written using Slater's approximation [17]. This energy functional is not the exact mean value of the Hamiltonian for a given independent particle state, but is only an approximation. It is interesting to note that this approximation has been tested for spherical nuclei [18], using the *SkP* and *SkM* forces and for *HFB* calculations using Gogny's force [19].

## 6. Angular Velocity

The static moment of inertia is defined as a function of the angular velocity corresponding to a spin  $I$ :

$$\Omega(I) = \frac{J}{\mathfrak{I}} = \frac{dE}{dJ}, \quad (21)$$

where  $\mathfrak{I}$  is the moment of inertia and  $\Omega$  is the angular velocity. The observation of the spectra of energy as a function of spin can reveal the rotational behavior of the nucleus. By analogy with the energy of a rigid body of moment of inertia  $\mathfrak{I}$  in rotation, we obtain:

$$E(I) = \frac{\hbar^2}{2\mathfrak{I}} I(I+1). \quad (22)$$

Two comparable quantities of the macroscopic moment of inertia can be defined; the moment of dynamic inertia and the moment of cinematic inertia [20-22],

$$\hbar\Omega = \left( \frac{\Delta E}{\Delta \sqrt{I(I+1)}} \right)_{(I,I-2)} \cong \left( \frac{E_\gamma}{\Delta I} \right)_{(I,I-2)} = \frac{E_\gamma}{2}, \quad (23)$$

which can be used to measure the energy of excitation of the spin level. In the following, we will investigate the evolution of the moment of inertia as a function of the angular velocity. This research is carried out in the experimental study through defining the angular velocity  $\Omega_I$  and the kinematical moment of inertia  $\mathfrak{I}^1$ , associated with a given rotational state of angular momentum  $I$ , through the transition energies  $E_{I \rightarrow I-2}$ ; namely,

$$\Omega_{\text{exp}}(I) = \frac{E_\gamma^+(I) + E_\gamma^-(I)}{4}. \quad (24)$$

The experimental static moment of inertia (in unit of  $\hbar^2 \text{MeV}^{-1}$ ) is written as follows:

$$\mathfrak{I}_{\text{exp}}^1 = \frac{4\sqrt{I(I+1)}}{E_\gamma^+(I) + E_\gamma^-(I)}, \quad (25)$$

where  $I$  is the projection on the intrinsic axis ( $Oz$ ) of the total angular momentum and  $E_\gamma^+(I), E_\gamma^-(I)$  are the transition energies before and after the considered energy level  $E(I)$ , which are given by the following relations:

$$E_\gamma^+ = E(I+2) - E(I); E_\gamma^- = E(I) - E(I-2). \quad (26)$$

The values of the experimental energies  $E(I)$  of the energy levels  $2+$  and the experimental static moments of inertia are traced in relation with the angular velocity, as illustrated in Fig. 4.

$$\hbar\Omega(I) = \frac{E_{I+2} - E_{I-2}}{4}. \quad (27)$$

## 7. Results and Discussion

We used the (HF + BCS) approach due to its advantage in that we study the static properties of these nuclei and deduce from this initial study the minimum deformation energy corresponding to the quadrupole moment.

The conditions for the HF + BCS calculation are as follows:

- We took an actual interaction from Skyrme SIII [23].
- We took a size of the base  $N_0=12$

of the axially symmetric harmonic oscillator (BOHSA). This size of the base is sufficient to have an energy of the fundamental close to the experimental value. In addition, it allows self-consistent calculations to be made in reasonable time.

We used a seniority force  $qg$  defined by the usual prescription which consists of a normalization of the intensity of the seniority force, noted  $G$ , with respect to the number of nucleons:

$$g = \frac{G}{11+N}$$

with  $N$  being the number of nucleons. The values of  $nG$  and  $pG$  that we have taken were determined by the authors of Ref. [24] by comparing the calculated minimal quasi-particle energies with those obtained from the experimental binding energies [25] using the 5-point formula [26].  $G_n = 16.50$  MeV,  $G_p = 15.50$  MeV.

Also, according to Ref. [24], the value of the BCS excitation window is taken to be equal to 5 MeV, in order to be able to compare our results with those of the authors of this reference.

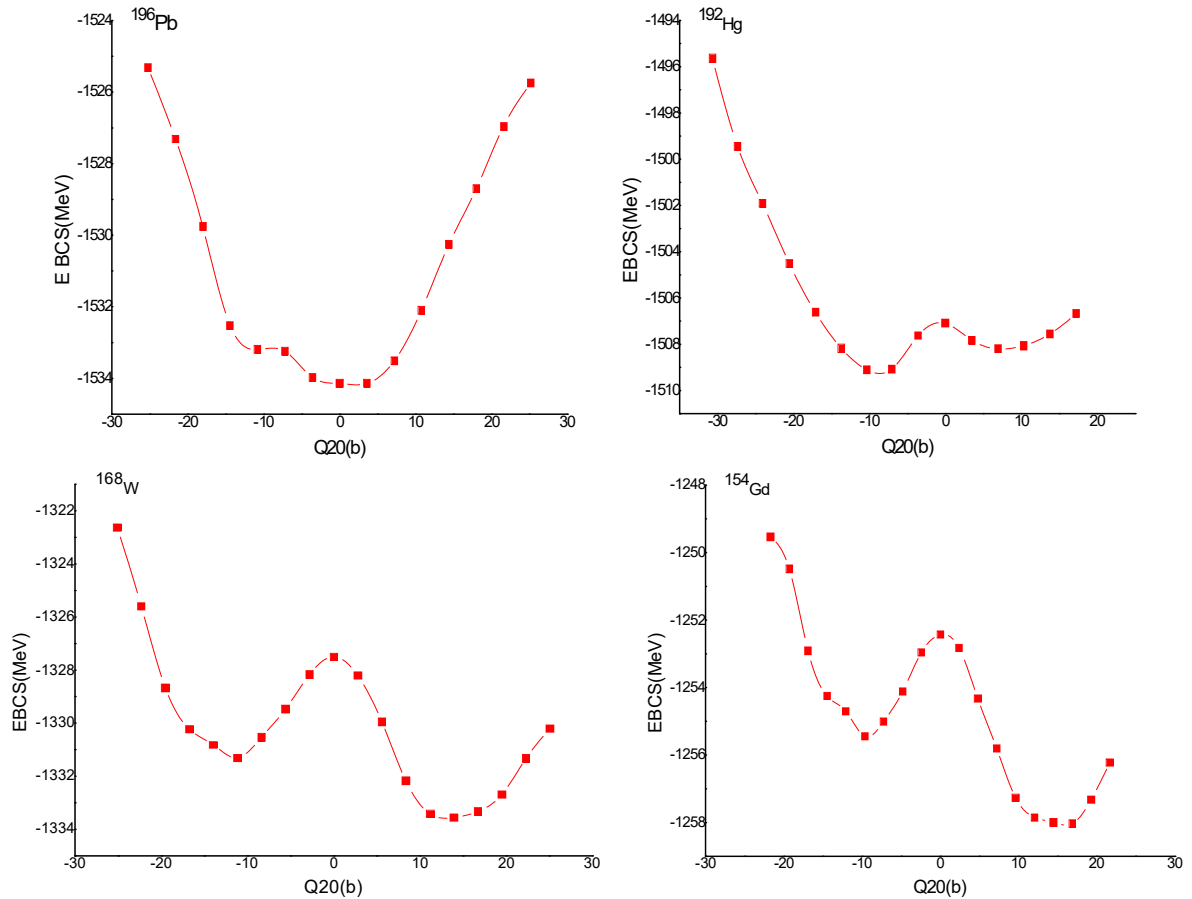


FIG. 1. Deformation-energy curves as a function of the quadrupole moment (in barns).

TABLE 1. Static properties of the four nuclei studied with the HF + BCS approach.

Nucleus	$E_{g,s}$ (MeV)	$E_{exp}$ (MeV)
$^{154}\text{Gd}$	-1258.15	-1266.61
$^{168}\text{W}$	-1334.66	-1342.98
$^{196}\text{Pb}$	-1533.51.66	-1539.51
$^{192}\text{Hg}$	-1508.20	-1519.10

We have chosen to study in detail this rotational-band model of a nucleus for some rare-earth isotopes. For reasons, which will become clear later, we have discussed the use of the Routhian Hartree-Fock method for isotopes of the nuclei Gd, W, Pb and Hg using the Routhian approximation. The existence of deformed stable nuclei has been demonstrated very early in the history of nuclear physics. The observation of large quadrupole moments leads to suggest that these nuclei have the shape of an elongated ellipsoid, which has been confirmed by the observation of rotational bands. The description of most nuclei as having axial deformation and being reflective asymmetrical about a plane perpendicular to the axis of symmetry is generally adequate to reproduce their nuclear spectra. As we said previously in Section 2, the Routhian of the system is obtained by adding a constraint on the angular momentum along the x1 axis in the Hamiltonian of the system. We have determined some rotational properties; namely, the rotational band in the ground state and the rotational velocity. We carried out the calculations with the Skyrme force SkM\* and we compared the results with the experimental data.

In Figs. (3 and 4), we have represented the variation of the collective angular velocity of rotation  $\Omega$  as a function of the spin I of the nuclei for the Skyrme force SkM\* that we compare with the experimental data. As well, the experimental velocity is defined above.

In Fig. 2, for the two nuclei (Hg and Pb) of the moment of inertia  $\mathfrak{S}^1$  as a function of angular velocity ( $\Omega$ ), the results are shown for four approaches (HF, HFB, HTDA and Cr.RHF) and these values are compared with the experimental results, where we notice that the HFB approach at low angular velocity behaves well, whereas in the HF approach, the values obtained were far from the experimental values; it is considered a rather weak approach, which led to the use of the HTDA approach, which showed a uniform behavior from the beginning to the top, compared to the HFB approach which had jumps at higher angular velocities. As for the approach used, Cr.RHF, which is an addition to the calculations of Routhian Hartree-Fock, where the calculations of the microscopic rotation, with conservation from the beginning, the number of particles (the BCS approach), provides an approach that can be followed. This approach has proven effectiveness in comparison with other approaches and studies. It gave good behavior from the beginning to the top and its results are close to the experimental results, but we notice some bending and divergence when increasing angular velocity, which is due, as is known in some nuclei, to the collective difference in coupling and since the approach is characterized by regular behavior, it is necessary that the bending will not appear in it, such as in  $^{154}\text{Gd}$  and  $^{164}\text{W}$  nuclei. We note that there is complete agreement of the  $^{156}\text{Gd}$ ,  $^{168}\text{W}$  and  $^{192}\text{Hg}$  nuclei up to the high spin I = 18 hbar.

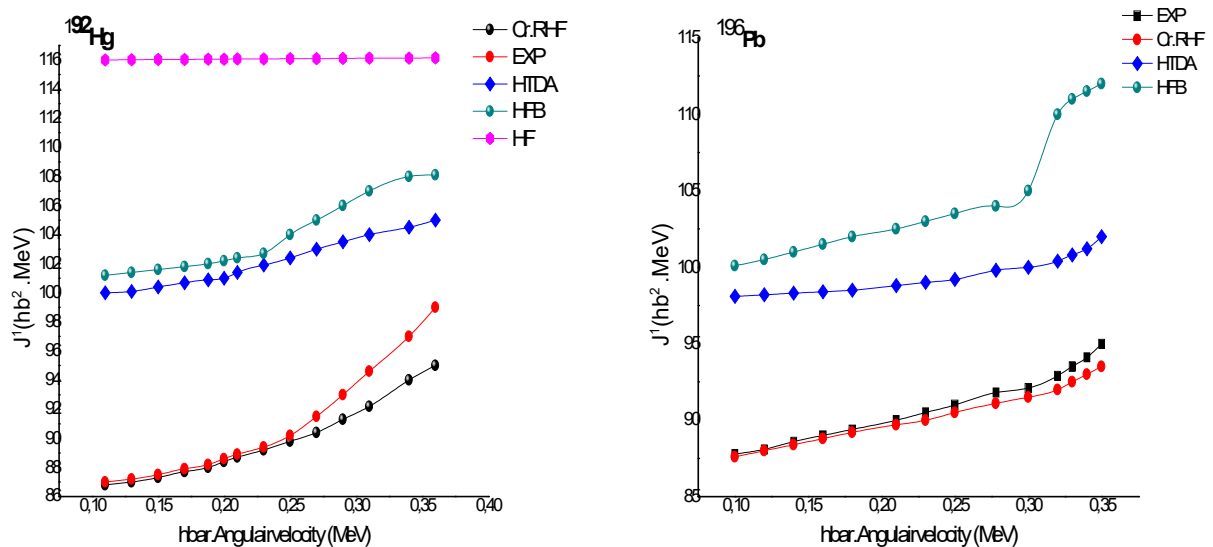


FIG. 2. Comparison between the moment of inertia  $\mathfrak{S}^1$  as a function of the angular velocity  $\Omega$  as obtained in the approaches HF, HFB, HTDA and Cr.RHF with the experimental results.

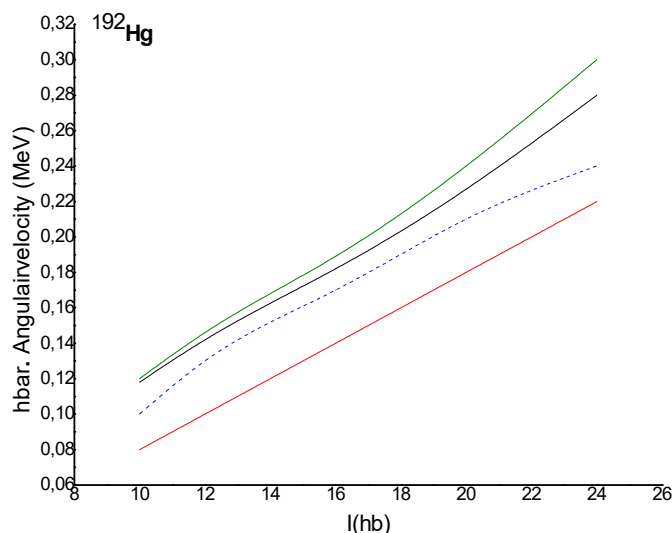


FIG. 3. Angular velocity as a function of the angular momentum  $I$  (in  $\hbar$  units). The conventions in use are the following: HFB value (dotted line), EXP value (green solid line), HF value (red solid line) and Cr.HF value (black solid line).

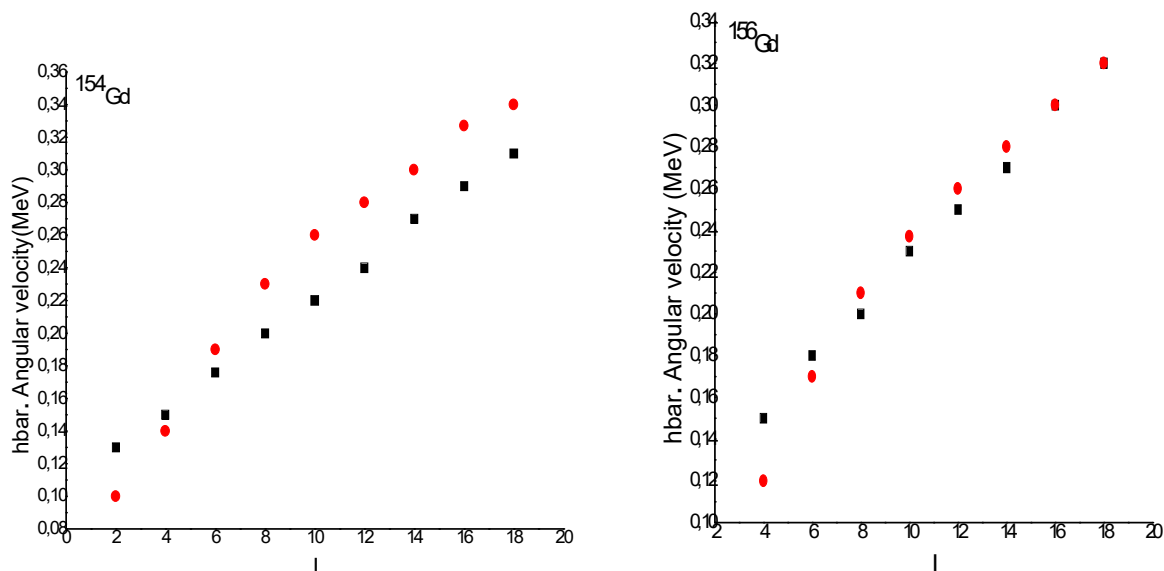


FIG. 4. Angular velocity as a function of the angular momentum and the experimental data (red circles).

The angular velocities within the three studied approaches HF, HFB and Cr.RHF are plotted in Fig. 3 against the angular momentum. We note that the Cr.RHF approach is close to the experimental results and it is well smooth compared to the HFB and HF approaches, which were not effective even at low angular velocities, as the results were found to be nearly compatible with a high rotation of up to 20 hbar, since it was compared in the Hg nucleus with the two approaches. Then, we were able to calculate the nuclei at  $A = 160$ ,  $A = 190$ . The linear behavior is observed up to spin  $I = 2\hbar \rightarrow 10\hbar$ . We observe an agreement of the angular velocity of the Cr.RHF model and that of the experiment. More precisely, we say that between  $I = 2\hbar$

and  $10\hbar$ , we found good results for the nuclei *Gd*, *W* and Hg which agree with the experimental results, as seen in Fig. 4. In addition, we obtained the angular momentum of the nucleus  $^{156}\text{Gd}$ , which is  $I = 10\hbar$  at the angular velocity  $0.23\text{MeV}\cdot\hbar^{-1}$ .

In Fig. 6, we have presented the collective states of rotation within the framework of the approximation of ellipsoids of type  $-S$ . Note also that the curve deduced with the force SKM\* is closer to the experimental curve than that deduced with the force SIII for the nucleus  $^{164}\text{Gd}$ . This means that the SKM\* force translates the rotation in the nucleus in a more realistic way. The rotational energy curves are located above the experimental curve.

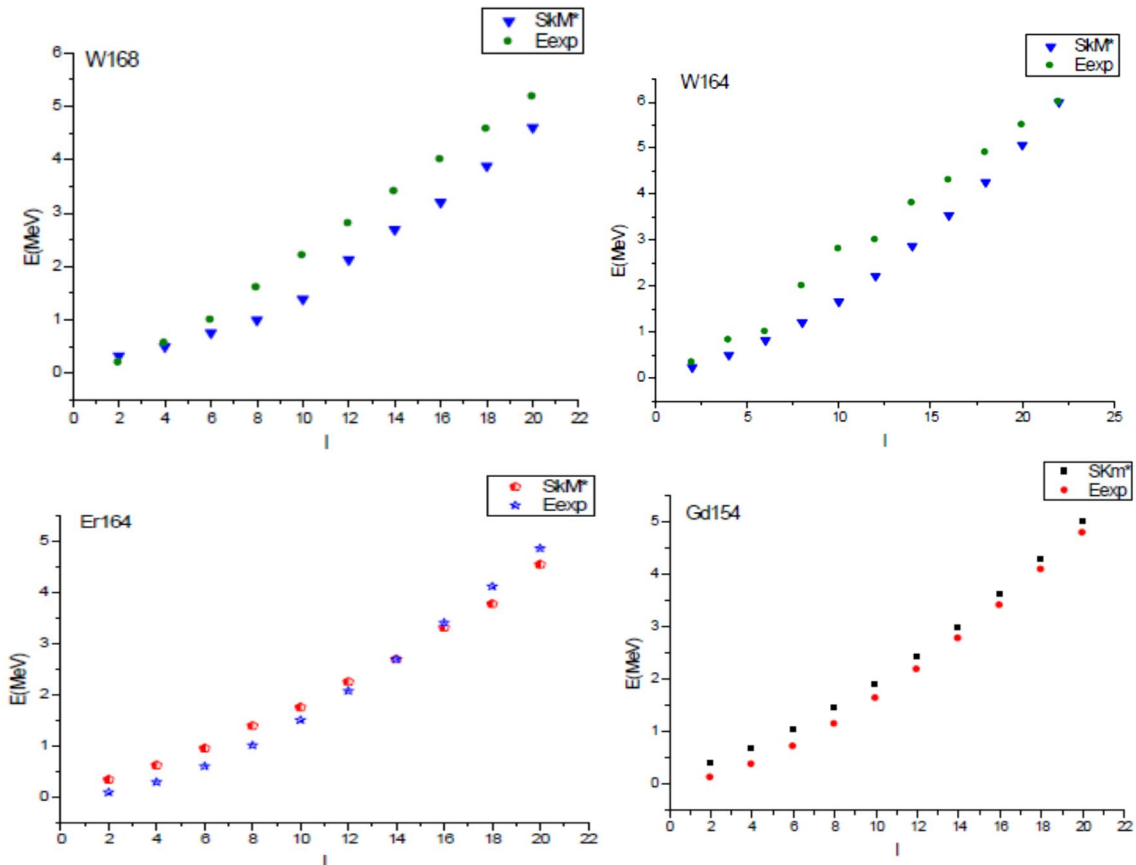


FIG. 5. The energy of the rotational state as a function of the spin.

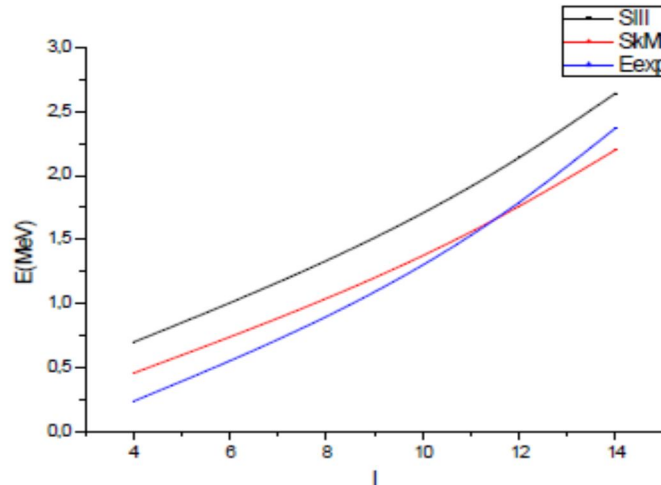


FIG. 6. The energy of the rotational state as a function of the spin with the two forces of Skyrme SIII and SkM\* for the nucleus  $^{164}Gd$ .

The experimental rotational energy as a function of the angular velocity in the results of HFR gives a rather smooth behavior, in reasonable agreement with the data at low angular velocities. However, at higher angular velocities, the results differ from the experimental ones. These differences, which are due to the sudden variations in the matching properties, do not appear in the RHF results that

show a regular behavior, in good qualitative agreement with the data. If we compare these results with the results of the HFB model, which are far from the experiment, in Ref. 55, as well as comparing them with the results of Ref. 22, which used the HTDA model, we conclude that with a static study using the (HF + BCS) model and by approximating the RHF, the results of the approach are close to the experiment.



## 8. Summary and Perspectives

In this paper, we have discussed some properties of static nuclei Gd, W, Pb and Hg, applying as the first study the approximation of HF+BCS and then the Cr. RHF approximation.

The new approach discussed here opens the door to a wide field of investigation. In particular, it offers a theoretical framework in which the even nuclei (odd-odd and odd-even) could be described in a coherent way. An unbalanced breakdown could also be envisaged in the same frame. In our opinion, the most important task to be accomplished would be to expand the space of many functions of the body

waves to improve the description of the correlations. Another important issue is the investigation of high-spin states. It is well known that the usual cranked HFB formalism does not see the proton-neutron pairing and is not very efficient in the low-pairing regime, which leads to discrepancies in the measured and the calculated yarest bands. As we mentioned, the treatment of the pairing correlations in high spins in the RHF method was already undertaken. Since the rotation has a different impact on like-particle and proton-neutron pairs, it may be judicious to enrich the RHF by including the proton-neutron coupling.

## References

- [1] Yuldashbaeva, E.K., Libert, J., Quentin, P. and Girod, M., Phys. Lett. B, 461 (1999) 1.
- [2] Pillet, N., Quentin, P. and Libert, J., Nucl. Phys. A, 697 (2002) 141.
- [3] Gall, B., Bonche, P., Dobaczewski, J. et al., Z. Phys. A, 348 (1994) 183.
- [4] Girod, M., Delaroche, J.P., Berger, J.F. and Libert, J., Phys. Lett. B, 325 (1994) 1.
- [5] Bardeen, J., Cooper, L.N. and Schrieffer, J.R., Phys. Rev., 108 (1957) 1175.
- [6] Parry, W.E., "The Many-body Problem", (Clarendon Press, Oxford, 1973).
- [7] Madland, D.G. and Rayford Nix, J., Nucl. Phys. A, 476 (1988) 1.
- [8] Vautherin, D. and Brink, D.M., Phys. Rev. C, 5 (1972) 626.
- [9] Waroquier, M., Heyde, K. and Wenes, G., Nucl. Phys. A, 404 (1983) 269.
- [10] Dutta, A.K. and Kohno, M., Nucl. Phys. A, 349 (1980) 455-79.
- [11] Prochniak, L., Quentin, P. and Imadalou, M., Int. J. Mod. Phys. E, 21 (2012) 1250036.
- [12] Chabanat, E., Bonche, P., Haensel, P., Meyer, J. and Schaeffer, R., Nucl. Phys. A, 627 (1997) 710-74.
- [13] Wiringa, R.B., Fiks, V. and Fabrocini, A., Phys. Rev. C, 38 (1988) 1010.
- [14] Engel, Y.M., Brink, D.M., Geoeke, K., Krieger, S.J. and Vautherin, D., Nucl. Phys. A, 249 (2) (1975) 215.
- [15] Bencheikh, K., Quentin, P. and Bartel, J., Nucl. Phys. A, 571 (1994) 518.
- [16] Slater, J.C., Phys. Rev. C, 81 (1951) 85.
- [17] Gombas, P., Ann. Phys., 10 (1952) 253.
- [18] Pillet, N., Quentin, P. and Libert, J., Nucl. Phys. A, 697 (2002) 14.
- [19] Inglis, D.R., Phys. Rev., 96 (1954) 1059.
- [20] Bartel, J., Quentin, P., Brack, M., Guet, C. and Haakansson, H.B., Nucl. Phys. A, 386 (1982) 79.
- [21] Laftchiev, H., Samsøen, D., Quentin, P. and Mikhailov, I.N., Phys. Rev. C, 67 (2003) 014301.
- [22] Laftchiev, H., Libert, J., Quentin, P. and Long, H.T., Nucl. Phys. A, 845 (2010) 33.
- [23] Beiner, M., Flocard, H., Van Giai, N. and Quentin, P., Nucl. Phys. A, 238 (1975) 29.
- [24] Próchniak, L., Quentin, P., Samsøen, D. and Libert, J., Nucl. Phys. A, 730 (2004) 59.
- [25] Audi, G. and Wapstra, A.H., Nucl. Phys. A, 595 (1995) 409.
- [26] Kumar, K. and Baranger, M., Nucl. Phys. A, 92 (1967) 608.